doi:10.1093/brain/awx015 BRAIN 2017: 140; 914–927 | 914

BRAIN
A JOURNAL OF NEUROLOGY

Rewiring the primary somatosensory cortex in carpal tunnel syndrome with acupuncture

Yumi Maeda,[1,2,*] Hyungjun Kim,[1,3,*] Norman Kettner,[2] Jieun Kim,[1,3] Stephen Cina,[1] Cristina Malatesta,[4] Jessica Gerber,[1] Claire McManus,[4] Rebecca Ong-Sutherland,[4] Pia Mezzacappa,[1] Alexandra Libby,[1] Ishtiaq Mawla,[1] Leslie R. Morse,[5] Ted J. Kaptchuk,[6] Joseph Audette[7] and Vitaly Napadow[1,2]

*These authors contributed equally to this work.

Carpal tunnel syndrome is the most common entrapment neuropathy, affecting the median nerve at the wrist. Acupuncture is a minimally-invasive and conservative therapeutic option, and while rooted in a complex practice ritual, acupuncture overlaps significantly with many conventional peripherally-focused neuromodulatory therapies. However, the neurophysiological mechanisms by which acupuncture impacts accepted subjective/psychological and objective/physiological outcomes are not well understood. Eligible patients ($n = 80$, 65 female, age: 49.3 ± 8.6 years) were enrolled and randomized into three intervention arms: (i) verum electro-acupuncture 'local' to the more affected hand; (ii) verum electro-acupuncture at 'distal' body sites, near the ankle contralesional to the more affected hand; and (iii) local sham electro-acupuncture using non-penetrating placebo needles. Acupuncture therapy was provided for 16 sessions over 8 weeks. Boston Carpal Tunnel Syndrome Questionnaire assessed pain and paraesthesia symptoms at baseline, following therapy and at 3-month follow-up. Nerve conduction studies assessing median nerve sensory latency and brain imaging data were acquired at baseline and following therapy. Functional magnetic resonance imaging assessed somatotopy in the primary somatosensory cortex using vibrotactile stimulation over three digits (2, 3 and 5). While all three acupuncture interventions reduced symptom severity, verum (local and distal) acupuncture was superior to sham in producing improvements in neurophysiological outcomes, both local to the wrist (i.e. median sensory nerve conduction latency) and in the brain (i.e. digit 2/3 cortical separation distance). Moreover, greater improvement in second/third interdigit cortical separation distance following verum acupuncture predicted sustained improvements in symptom severity at 3-month follow-up. We further explored potential differential mechanisms of local versus distal acupuncture using diffusion tensor imaging of white matter microstructure adjacent to the primary somatosensory cortex. Compared to healthy adults ($n = 34$, 28 female, 49.7 ± 9.9 years old), patients with carpal tunnel syndrome demonstrated increased fractional anisotropy in several regions and, for these regions we found that improvement in median nerve latency was associated with reduction of fractional anisotropy near (i) contralesional hand area following verum, but not sham, acupuncture; (ii) ipsilesional hand area following local, but not distal or sham, acupuncture; and (iii) ipsilesional leg area following distal, but not local or sham, acupuncture. As these primary somatosensory cortex subregions are distinctly targeted by local versus distal acupuncture electrostimulation, acupuncture at local versus distal sites may improve median nerve function at the wrist by somatotopically distinct neuroplasticity in the primary somatosensory cortex following therapy. Our study further suggests that improvements in primary somatosensory cortex somatotopy can predict long-term clinical outcomes for carpal tunnel syndrome.

1 Athinoula A. Martinos Center for Biomedical Imaging, Department of Radiology, Massachusetts General Hospital, Charlestown, MA, 02129, USA
2 Department of Radiology, Logan University, Chesterfield, MO, 63017, USA
3 Clinical Research Division, Korean Institute of Oriental Medicine, Daejeon, 34054, South Korea
4 Department of Physical Medicine and Rehabilitation, Spaulding Rehabilitation Hospital, Medford, MA, 02155, USA

Received August 11, 2016. Revised December 8, 2016. Accepted December 17, 2016. Advance Access publication March 2, 2017

5 Department of Physical Medicine and Rehabilitation, Harvard Medical School, Spaulding Rehabilitation Hospital, Boston, MA, 02114, USA
6 Department of Medicine, Beth Israel Deaconess Medical Center, Boston, MA 02215, USA
7 Department of Pain Medicine, Harvard Vanguard Medical Associates, Atrium Health, Boston, MA, 02215, USA

Correspondence to: Vitaly Napadow, PhD,
Martinos Center for Biomedical Imaging,
#2301 149 Thirteenth St.,
Charlestown, MA 02129,
USA
E-mail: vitaly@nmr.mgh.harvard.edu

Keywords: carpal tunnel syndrome; nerve conduction studies; neuropathic pain; entrapment neuropathy; neuromuscular disease: imaging

Abbreviations: BCTQ = Boston Carpal Tunnel Syndrome Questionnaire; CTS = carpal tunnel syndrome; DTI = diffusion tensor imaging; S1 = primary somatosensory cortex

Introduction

Entrapment neuropathies are common sources of pain and paraesthesia (Neal and Fields, 2010), and entrapment of the median nerve at the wrist, termed carpal tunnel syndrome (CTS), accounts for 90% of such neuropathies (Atroshi *et al.*, 1999; Papanicolaou *et al.*, 2001; Kleopa, 2015). Prior to surgical approaches for severe CTS, conservative therapies are commonly recommended (Kleopa 2015), and acupuncture has been proposed as a viable option (Yang *et al.*, 2009). Acupuncture is a minimally-invasive therapeutic modality that originated in China 2000 years ago as a component of traditional Chinese medicine (Kaptchuk, 2002). While acupuncture therapy is rooted in a complex practice ritual, the acupuncture needle procedure, particularly when coupled with electrical needle stimulation, overlaps significantly with many conventional peripheral neuromodulatory therapies (Langevin *et al.*, 2015) that have generated significant excitement as 'electroceuticals' targeting peripheral nerve receptors (Famm *et al.*, 2013; Waltz, 2016). However, the neurophysiological mechanisms by which acupuncture impacts subjective/psychological (i.e. symptom report) and objective/physiological (e.g. median nerve conduction studies) outcomes in CTS are not well understood.

Previous neuroimaging studies have demonstrated that while CTS results from compression of the median nerve at the wrist, this disorder is also characterized by structural (Maeda *et al.*, 2013*a*, 2016) and functional (Druschky *et al.*, 2000; Tecchio *et al.*, 2002; Napadow *et al.*, 2006; Dhond *et al.*, 2012; Maeda *et al.*, 2014) neuroplasticity in the primary somatosensory cortex (S1) of the brain. Specifically, CTS patients show decreased S1 grey matter volume and cortical thickness contralateral to the more affected hand, which is further pronounced in paraesthesia-dominant symptom subgroups (Maeda *et al.*, 2016), and is associated with aberrant median nerve conduction (Maeda *et al.*, 2013*a*, 2016). Functional MRI evaluation has demonstrated reduced separation between S1 cortical representations of adjacent median nerve innervated fingers, digits 2 and 3 (D2/D3)—a reproducible finding in different CTS cohorts, using both functional MRI (Napadow *et al.*, 2006; Maeda *et al.*, 2014) and MEG (Dhond *et al.*, 2012). Interestingly, reduced D2/D3 separation in S1 has been associated with median sensory nerve conduction latency (Napadow *et al.*, 2006), symptom severity, reduced fine motor performance, and diminished sensory discrimination accuracy (Maeda *et al.*, 2014), demonstrating that such functional brain neuroplasticity is indeed maladaptive.

Acupuncture was suggested as a promising adjunct therapy for CTS at the 1997 NIH consensus conference, organized to critically evaluate acupuncture research (NIH 1998). Since then, randomized controlled trials have found improved nerve conduction and reduced symptom severity following acupuncture, compared to either sham acupuncture (Khosrawi *et al.*, 2012) or oral steroids (Yang *et al.*, 2009, 2011). Other trials have not found symptom severity reduction (Yao *et al.*, 2012) following acupuncture. Importantly, while later Yao *et al.* trials did not confirm CTS by nerve conduction studies and likely enrolled both CTS and idiopathic hand pain patients, the earlier Yang *et al.* trials did enrol based on conduction latency (Yang *et al.*, 2009), and evaluated long-term follow-up (Yang *et al.*, 2011). A meta-analysis, performed prior to some of the recent trials, noted encouraging but not yet convincing evidence for acupuncture in the treatment of CTS (Sim *et al.*, 2011), advocating for more randomized controlled trials.

Our multi-modal randomized neuroimaging trial follows-up on our smaller ($n = 13$) and uncontrolled (no sham acupuncture) pilot imaging study assessing acupuncture outcomes for CTS (Napadow *et al.*, 2007*a*). The current study assessed whether (i) verum acupuncture is superior to sham acupuncture for reducing symptom severity, improving median nerve conduction latency, and increasing functional MRI-assessed D2/D3 separation distance in S1; (ii) verum acupuncture at distal acupoints (i.e. no local needle-induced physiological response) is also superior to

sham acupuncture; (iii) improvements in physiological outcomes immediately following verum acupuncture predict long-term symptom reduction; and (iv) neuroplasticity in S1-adjacent white matter microstructure, as assessed by diffusion tensor imaging (DTI), can also inform potential brain-based mechanisms by which local versus distal acupuncture improves CTS outcomes. We hypothesized that while both verum and sham acupuncture reduce CTS symptom severity, only verum acupuncture improves physiological outcomes and such changes predict long-term clinical outcomes. Moreover, we hypothesized that improvement in median nerve conduction after acupuncture is associated with plasticity in somatotopically-specific S1-adjacent white matter microstructure targeted by local versus distal acupuncture.

Materials and methods

Experimental design

This was a single-centre, blinded, placebo controlled, randomized parallel-group longitudinal neuroimaging study, pre-registered with ClinicalTrials.gov (NCT01345994). The study took place at Spaulding Rehabilitation Hospital (SRH) and Athinoula A. Martinos Center for Biomedical Imaging, Department of Radiology, Massachusetts General Hospital (MGH), in Boston, MA from January 2009 to December 2014. All study protocols were approved by MGH and Partners Human Research Committee and all subjects provided written informed consent.

Subjects

Patients with CTS, 20–65 years old, were recruited at MGH and SRH. Subjects were consented and evaluated by study physician (blinded to allocation), who captured history of symptoms, examination for Phalen's manoeuvre (Phalen, 1966) and Durkan's sign (Durkan, 1991), and nerve conduction studies (Cadwell Sierra EMG/NCS Device). The latter evaluated median and ulnar, sensory and motor nerve conduction for both hands. Inclusion criteria for mild/moderate CTS subjects required a history of pain/paraesthesia in median nerve innervated territories, greater than 3 months duration, median sensory nerve conduction latency >3.7 ms for mild CTS, >4.2 ms for moderate CTS, and/or >0.5 ms compared to ulnar sensory nerve latency for both mild and moderate CTS, with normal motor conductions. Subjects with >4.2 ms median nerve motor latency and $>50\%$ loss of motor amplitudes were considered to be 'severe' and excluded from this study. For subjects diagnosed with bilateral CTS, the more affected hand, by symptom report, was used for primary outcomes. Exclusion criteria were as follows: contraindications to MRI, history of diabetes mellitus, rheumatoid arthritis, wrist fracture with direct trauma to median nerve, current usage of prescriptive opioid medication, severe thenar atrophy, previous acupuncture treatment for CTS, non-median nerve entrapment, cervical radiculopathy or myelopathy, generalized peripheral neuropathy, severe cardiovascular, respiratory, or neurological illnesses, blood dyscrasia or coagulopathy or current use of anticoagulation therapy. Healthy control subjects, 20–65 years old, were also recruited for baseline neuroimaging comparisons.

Study timeline

Following baseline clinical and MRI assessment, eligible subjects were randomly assigned to one of three parallel study arms (Fig. 1). We used computer generated permuted block randomization (blocks of six), stratified by CTS severity (mild/moderate). The acupuncturist was informed of group allocation at the first treatment visit. The three intervention arms were (i) verum acupuncture 'local' to the more affected hand; (ii) verum acupuncture at 'distal' body sites, contralesional to the more affected hand; and (iii) sham acupuncture using non-penetrating placebo needles. Brain MRI scans were obtained at baseline and post-therapy. Nerve conduction studies were obtained at baseline and after acupuncture therapy while symptom severity, assessed with the Boston Carpal Tunnel Syndrome Questionnaire, BCTQ (Levine *et al.*, 1993), was additionally assessed at 3-month follow-up (see below).

Acupuncture treatment

Subjects received 16 acupuncture treatments over 8 weeks using a tapering schedule common to the clinic: three treatments/week for 3 weeks; two treatments/week for 2 weeks; and one treatment/week for 3 weeks. Acupuncture was delivered to subjects in supine position by one of four trained, licensed acupuncturists with at least 3 years of clinical experience. For the local acupuncture group, based on the protocol used in our pilot study (Napadow *et al.*, 2007*b*), a hybrid design balanced standardized acupuncture therapy with more ecologically valid individualized acupoint selection. For all subjects, acupuncture needles were placed at acupoints TW5 and PC7 (Fig. 1 for all point locations), on the dorsal and ventral aspects of the forearm of the more affected hand. Electrodes were attached to these needles, and 2 Hz electrical stimulation was performed for 20 min using a constant-current electro-acupuncture device (Acus II, Cefar). Current intensity was set to a percept level of 'moderately strong but not painful.' Acupuncture needles were also inserted, and manually stimulated, at three additional acupoints on the more affected forearm, chosen by the acupuncturist from HT3, PC3, SI4, LI5, LI10, and LU5, according to subjects' individual presentation. Manual stimulation at all locations was performed to induce characteristic *deqi* acupuncture sensation (Kong *et al.*, 2007). For the distal acupuncture group, electro-acupuncture was performed with needles placed at SP6 and LV4 on the lower leg on the opposite side of the body to the more affected hand. Manual acupuncture was also performed at three additional acupoints: GB34, KD3, and SP5 on this limb. All verum acupuncture needles were single-use disposable needles (0.20–0.25 mm diameter, 20–40 mm length, stainless steel needle; Asiamed) inserted 10–30 mm deep, depending on location. Additionally, to maintain credibility for this procedure, a single non-insertive sham acupuncture needle (Streitberger Needle; Asiamed) was placed at non-acupoint SH1 on the forearm of the more affected hand. For the sham acupuncture group, non-insertive Streitberger needles were placed on non-acupoints (SH1 and SH2) on the ulnar aspect of the more

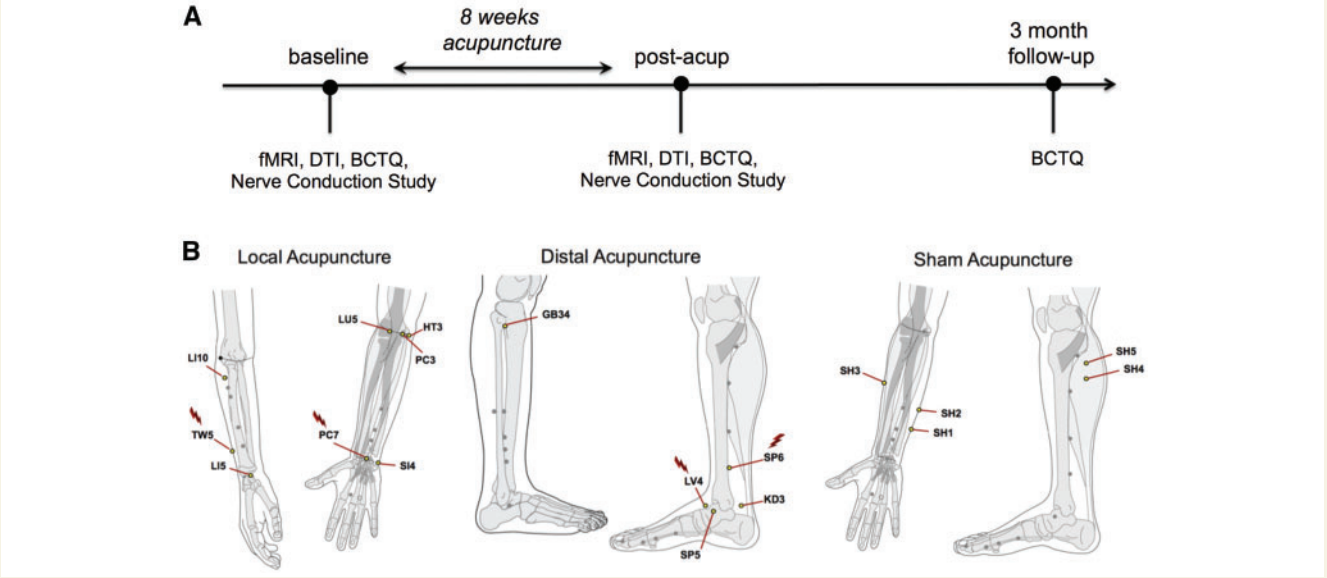

Figure 1 Study overview. (**A**) Study design of randomized control neuroimaging trial with acupuncture intervention; multi-modal assessments were conducted at baseline, post-acupuncture, and 3-month follow-up. (**B**) Location of acupoints for all three study arms: local (verum, near the more affected hand), distal (verum, near contralesional ankle), and sham (non-penetrating needles over non-acupoints near the more affected hand). Acupoints where electrical stimulation was provided via electrodes attached to needles (i.e. electro-acupuncture) are marked (lightning bolt). fMRI = functional MRI.

affected forearm. Similar to the local verum acupuncture arm, electrodes were attached to these needles, the electro-acupuncture device was turned on, but the electrodes were not inserted into an active port on the device. Subjects were told they 'may or may not feel electrical sensations' from this procedure. Additionally, three other sham needles were placed over non-acupoints SH3 on the radial aspect of the more affected forearm, and non-acupoints SH4, SH5 on the opposite lower limb. Throughout the evaluation and treatment period, subjects, study physician, and experimenters were blinded to group allocation and all data capture forms used neutral group codes to conceal allocation: 'ektorp,' 'klobo,' 'poang.' Subjects' perception of whether they received active acupuncture therapy was assessed after the first treatment. After the post-therapy MRI visit, subjects were unblinded as to group allocation.

Clinical outcomes

The BCTQ (Levine *et al.*, 1993) was administered at baseline, post-therapy, and at 3-month follow-up. It is composed of a symptom severity scale, which includes 10 items regarding pain and numbness severity, and an 8-item Function Severity Scale related to precise hand movement tasks using a 1–5 scale. The symptom severity scale served as the primary clinical outcome measure for symptom assessment.

Nerve conduction studies were performed according to previously described methods (Ma *et al.*, 1983), at baseline and post-therapy. Median sensory nerve conduction latency was calculated from the average of digit 2 (D2) and digit 3 (D3) measurements from the affected hand (more affected hand for bilateral CTS subjects).

MRI outcomes

S1 cortical mapping with functional MRI

At baseline and post-therapy, imaging data were acquired with a 3 T Siemens Trio equipped with a 32-channel head coil. Structural MRI data were acquired with a multi-echo MPRAGE T_1-weighted pulse sequence (repetition time = 2530 ms, echo time 1/echo time 2 = 1.64/30.0 ms, inversion time = 1200 ms, flip angle = 7°, field of view = 256 × 256, 176 slices, sagittal acquisition, spatial resolution = 1 × 1 × 1 mm^3). Functional MRI data were acquired using a gradient echo blood oxygen level-dependent T_2^*-weighted pulse sequence adapted for improved spatial resolution (repetition time/echo time = 2000/30 ms, field of view = 200 × 200 mm, 32 coronal slices parallel to the central sulcus, voxel size = 2.1 × 2.1 × 2.5 mm, flip angle = 90°). We used an event-related functional MRI design to evaluate brain response to vibrotactile stimulation over three digits (D2, D3, and D5) on the more affected hand. D2 and D3 are innervated by the median nerve (affected by CTS), while D5 is innervated by the unaffected ulnar nerve. Computer controlled vibrotactile stimulation was provided by a custom-built MR-compatible device as described in our previous study (Maeda *et al.*, 2014). In brief, the device contained four piezoelectric transducers (T220-A4NM-303Y, Piezo Systems) set inside an adjustable four-finger shell that allowed for directed vibrotactile stimulation to the distal finger pad provided by Cortical Metrics. Stimulation was produced with sinusoid input voltage from an analogue signal generator (HM8030_5, HAMEG Instruments), and transmission was set according to an event related schedule through electronic relays, controlled by

customized software (Labview 7.1, National Instruments Corporation). A separate functional MRI scan was performed for each of the three digits using an event-related design (27 stimuli, duration = 2 s, randomized jittered inter-stimulus interval = 6–12 s, total scan time = 306 s). The order of digit stimulation was also randomized. For all functional MRI scans, subjects lay supine in the scanner with ear plugs and were instructed to close their eyes and focus attention on the finger being stimulated during the scan. Following each scan, subjects reported which finger was stimulated and the intensity of stimulus perception on a scale of 0 (no sensation) to 10 (very strong but not painful) to confirm proper device operation and attentiveness during the scan.

Functional MRI data were analysed using previously described methods (Maeda *et al.*, 2014), and were automated, thus blind to group allocation. Briefly, functional MRI data were registered to each subject's structural data (bbregistration; Greve *et al.*, 2009; Freesurfer v.5.1). Preprocessing included slice-timing correction, head motion correction, skull stripping, high pass filtering (cut-off period = 90 s) and minimal spatial Gaussian smoothing (full-width at half-maximum = 1 mm, FSL v.4.1; Jenkinson *et al.*, 2012). Preprocessed functional MRI data were analysed with a general linear model (GLM).

To calculate group functional MRI response maps, the resultant parameter estimates and variances for each digit on the single subject level GLM were projected on to the average surface brain (fsaverage, Freesurfer) and smoothed on the spherical cortical surface (full-width at half-maximum = 5 mm, mri_vol2surf, mri_surf2surf, Freesurfer). CTS subjects whose more affected hand was the left and, thus, experienced finger stimulation on the left hand, had their functional and structural data flipped across the mid-sagittal plane to perform group analyses with right hand affected subjects, similar to our previous analyses (Napadow *et al.*, 2006, 2007*a*; Maeda *et al.*, 2013*a*, 2014). Accurate registration was ensured by visualization (tkmedit, tkregister, Freesurfer). Group maps were cluster corrected for multiple comparisons ($z = 2.3$, $P < 0.05$).

For region of interest analysis, an unbiased group activation map across all digits and all subjects was calculated and intersected with the Freesurfer anatomical postcentral gyrus label for Brodmann area 3b and 1 (BA3b/1) to better localize digit representations to subregions of S1 known to demonstrate more precise somatotopic organization. This region of interest mask was then used to localize the peak z-stat vertex within the most significant cluster for each subject (mri_surfcluster, Freesurfer v.5.1). The geodesic surface distance between pairs of peak z-stat vertices for D2, D3 and D5 was then calculated using an edge cost and Dijkstra's algorithm (mris_pmake, Freesurfer v.5.1). Based on our previous studies, the primary outcome for functional S1 plasticity was defined as post-acupuncture change in D2/D3 separation distance. D2/D5 and D3/D5 separation were also calculated as D5 is ulnar, not median, nerve innervated and can be used as a stable reference location (Napadow *et al.*, 2006, 2007a) to determine if, for example, increased D2/D3 separation was due to ventral shift in D2 or dorsal shift in D3.

Diffusion tensor imaging of S1-adjacent white matter

Diffusion-weighted images were also obtained using spin-echo pulse sequence (repetition time/echo time = 8040/84 ms, voxel size = 2 × 2 × 2 mm, 64 slices, b-value = 700 s/mm^2, 60 non-collinear directions, 10 $b_0$volumes). Diffusion-weighted images were aligned to the b_0 image using affine registration, which serves to correct distortion due to eddy currents. After removal of non-brain tissue, DTI metric (fractional anisotropy, and mean, radial and axial diffusivity) maps were computed from the diffusion-weighted images using FMRIB's DiffusionToolbox (FDT, FSL), which fits a diffusion tensor model to each voxel. Maps for patients with CTS whose more affected hand was the left hand were flipped across the mid-sagittal plane for group analyses with right hand affected subjects, similar to functional MRI analyses.

We adopted a longitudinal diffusion processing scheme similar to previous analyses (Douaud *et al.*, 2009; Engvig *et al.*, 2012). First, the initial alignment between brain-extracted images at baseline and post-treatment time points were conducted using FMRIB's Linear Image Registration Tool (FLIRT, degrees of freedom = 6), and both images were resampled to a common space halfway between the two (Jenkinson *et al.*, 2002), which only requires a single registration per volume and thus minimizes registration bias towards one of the two time points. Next, we averaged the two registered fractional anisotropy maps to generate a subject-wise mid-space template, and images were aligned to the FMRIB58_FA template using FMRIB's Nonlinear Registration Tool (Jenkinson *et al.*, 2012). The mean fractional anisotropy map was thinned and thresholded at fractional anisotropy > 0.2 to generate a white matter tract skeleton representing the centre of the tracts common to all subjects (Smith *et al.*, 2006). Each image was warped to the standard MNI space using these transformations, and skeletonized after spatial smoothing (full-width at half-maximum = 4 mm).

Statistical comparisons of the fractional anisotropy skeletons between healthy controls and patients were performed using a non-parametric permutation test ($n = 5000$ permutations). As age significantly correlated with mean skeleton fractional anisotropy at baseline ($r = -0.39$; $P = 0.002$) but sex did not ($P = 0.33$), age served as a covariate of no-interest. Significance threshold was set at $P < 0.05$, family-wise error (FWE) corrected for multiple comparisons across voxels using threshold-free cluster-enhancement (Randomise 2.0, FSL; Winkler *et al.*, 2014).

In addition, as previous studies have demonstrated specific neuroplasticity in S1 structure and function in patients with CTS (Napadow *et al.*, 2006; Maeda *et al.*, 2013*a*, 2016), analyses were focused on S1-adjacent white matter. This region of interest was defined by a dilated mask of the postcentral gyrus taken from the Harvard-Oxford atlas, and intersected with the white matter skeleton (Supplementary Fig. 1). Notably, this mask did not include the superior longitudinal fasciculus, located medial to S1-adjacent U-fibres, as it is difficult to interpret fractional anisotropy in crossing-fibre areas (Douaud *et al.*, 2011).

Statistical analyses

For assessment of change in BCTQ scores, nerve conduction studies, and digit separation distance, repeated measures

ANOVA were performed (IBM SPSS version 20, Chicago, IL) and Greenhouse–Geisser corrected for sphericity (when appropriate). When the results for local and distal acupuncture groups did not differ (non-significant Group × Time interaction), we combined data from these two groups to produce a single 'verum' acupuncture group, which was then compared with the sham acupuncture. *Post hoc* testing was two-tailed for verum versus sham contrasts, and single-tailed for follow-up individual group contrasts (e.g. local versus sham), when the verum versus sham contrast was significant or trending. While randomization was stratified by CTS severity (i.e. nerve conduction studies), other outcomes were not used to stratify randomization. As previous studies have found that % change scores, which effectively normalize difference scores by the baseline value, are less sensitive to baseline differences than absolute difference scores (Farrar *et al.*, 2001; Jensen *et al.*, 2003; Hanley *et al.*, 2006), the former were also used for BCTQ and functional MRI outcomes. Significance was set at alpha = 0.05.

Results

A total of 80 CTS subjects [65 female, age: 49.3 ± 8.6 years, mean ± standard deviation (SD)] were enrolled and 79 subjects with CTS were randomized into three acupuncture groups, local ($n = 28$, 22 female, age: 48.5 ± 10.1 years), distal ($n = 28$, 22 female, age: 49.9 ± 8.4 years), and sham ($n = 23$, 20 female, 50.6 ± 7.8 years). There was no significant difference in age or male/female distribution between groups [$F(2,76) = 0.37$, $P = 0.69$. Fisher's exact test, $P = 0.72$]. Symptom duration (local = 9.9 ± 8.9 years, distal = 6.8 ± 6.6 years, sham = 9.4 ± 9.3 years) also did not differ significantly between groups [$F(2,76) = 1.12$, $P = 0.33$]. Due to scheduling difficulties, a total of 65 subjects with CTS completed their post-therapy MRI evaluation, and 56 subjects completed the BCTQ at 3-month follow-up (Supplementary Fig. 2). No significant differences were found between local, distal, or sham groups in subjects' perception of whether they received active acupuncture, at baseline (Fisher's exact test, $n = 64$, $P = 0.29$) or after the final acupuncture session (Fisher's exact test, $n = 62$, $P = 0.51$), with ~85% of subjects across all groups reporting that they indeed thought they had received active acupuncture. To provide better context for DTI analyses, a cohort of 34 age- and sex-matched healthy control subjects (28 female, age = 49.7 ± 9.9 years) were included for comparison with CTS subjects (baseline comparisons for clinical and functional MRI metrics were previously reported) (Maeda *et al.*, 2014).

Boston Carpal Tunnel Syndrome Questionnaire

The primary clinical outcome for symptom assessment was the symptom severity scale for the BCTQ. As the BCTQ symptom severity scale correlated with age at baseline ($n = 80$, $r = -0.22$, $P = 0.046$) and differed by sex (female: $n = 65$, 2.8 ± 0.7, mean ± SD; male: $n = 15$, 2.3 ± 0.5, $P = 0.02$), subsequent analyses used a repeated measures analysis of covariance ANCOVA (factors: Time, Group), controlling for age and sex. Furthermore, as there was no significant Group (local, distal acupuncture) × Time (baseline, post-therapy, 3-month follow-up) interaction for the two verum acupuncture groups [$F(1.9,65.4) = 1.82$; $P = 0.17$], the local and distal acupuncture groups were merged into a single verum group for subsequent analyses. A repeated measure ANCOVA then found a trending significance [$F(2.0,102.2) = 2.39$; $P = 0.098$] for the Group (verum, sham) × Time (baseline, post-therapy, 3-month follow-up) interaction. *Post hoc* testing demonstrated that both verum (−21.3 ± 22.0%, mean ± SD, $P < 0.001$, one-sample *t*-test) and sham (−22.7 ± 22.6%, $P = 0.001$) acupuncture significantly reduced the BCTQ symptom severity scale score immediately following therapy (Fig. 2 and Table 1), and did not differ ($P = 0.92$) controlling for age and sex. Comparisons of baseline to 3-month follow-up showed significant per cent improvement was retained for verum (−25.1 ± 20.8%, $P < 0.001$) and only a trending improvement was retained for sham (−11.1 ± 24.7%, $P = 0.08$) acupuncture, with a significant difference between the two groups at follow-up ($P = 0.04$), controlling for age and sex. Within the verum acupuncture group, both local (−24.6 ± 22.2%, $P < 0.001$) and distal (−25.6 ± 19.7%, $P < 0.001$) acupuncture demonstrated a significant reduction of BCTQ symptom severity scale at the 3-month

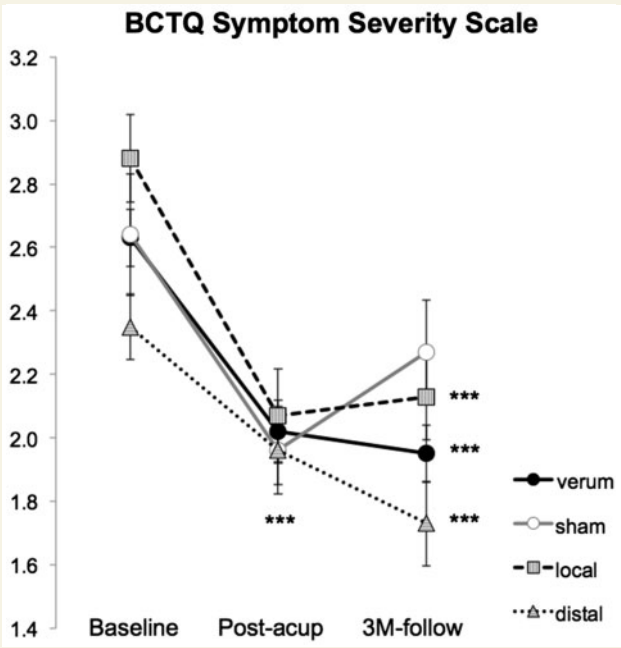

Figure 2 BCTQ response to therapy. Symptom assessment with the BCTQ symptom severity scale (SSS) demonstrated reduced symptom severity following all three acupuncture treatments. Note that CTS verum combines results across both CTS-local and CTS-distal study arms. Error bars represent standard error of the mean (SEM). ***$P < 0.001$.

Table 1 Demographics and clinical assessments

	Local acup	Distal acup	Sham acup	Verum versus sham *P*-value	Local versus sham *P*-value	Distal versus sham *P*-value
Age (years)	48.5 ± 10.1	49.9 ± 8.4	50.6 ± 7.8	0.53	0.42	0.77
Symptom duration (years)	9.9 ± 8.9	6.8 ± 6.6	9.4 ± 9.3	0.60	0.86	0.24
Change in BCTQ (Post-Acup − Baseline)						
Symptom severity score (%)	−27.0 ± 22.9	−14.7 ± 19.6	−22.7 ± 22.6	0.92	0.26	0.26
Function status score (%)	−26.2 ± 19.1	−6.8 ± 37.6	−18.2 ± 33.6	0.93	0.23	0.22
Change in BCTQ (3M − Baseline)						
Symptom severity score (%)	−24.6 ± 22.2	−25.6 ± 19.7	−11.1 ± 24.7	***0.04***	***0.04***	***0.04***
Function status score (%)	−16.8 ± 32.4	−17.4 ± 18.1	−2.3 ± 33.7	0.12	0.18	0.25
Change in median nerve conduction latency (Post-Acup − Baseline)						
Median sensory latency (ms)	−0.16 ± 0.42	−0.17 ± 0.35	0.12 ± 0.51	***0.02***	***0.03***	***0.02***
Change in S1 cortical separation distance (Post-Acup − Baseline)						
D2/D3 (mm)	2.3 ± 2.3	1.3 ± 3.9	−0.1 ± 3.2	*0.1*	***0.02***	0.18
D3/D5 (mm)	0.8 ± 5.3	−0.1 ± 3.4	−0.6 ± 2.6	0.48	0.40	0.69
D2/D5 (mm)	2.5 ± 4.0	1.3 ± 4.9	−0.1 ± 3.0	0.15	*0.07*	0.37

Data are shown as mean ± SD. Verum denotes combined local and distal acupuncture groups if local does not statistically differ from distal. Values in bold denote significance at $P < 0.05$; values in italics denote trending significance, which may help guide the design of future research.

follow-up. Results from the BCTQ functional scale are provided in Table 1.

Nerve conduction studies

The primary clinical outcome for nerve conduction studies was median sensory nerve conduction latency, which did not differ by sex, nor was correlated with age. Data from two subjects were unusable due to missing values. A 2 × 2 repeated measures ANOVA found no significant Group (local, distal acupuncture) × Time (baseline, post-therapy) interaction for the verum acupuncture groups [$F(1,40) = 0.01$, $P = 0.95$], and thus the local and distal acupuncture groups were merged into a single verum group for subsequent analyses. A repeated measures ANOVA for verum and sham acupuncture demonstrated a significant Group (verum, sham acupuncture) × Time (baseline, post-therapy) interaction [$F(1,61) = 6.25$, $P = 0.02$]. *Post hoc* testing found a significant difference for change in latencies between verum and sham acupuncture (unpaired *t*-test, $P = 0.02$; Fig. 3 and Table 1). Furthermore, a significant reduction for median sensory nerve latency was found following verum acupuncture (−0.16 ± 0.38 ms, mean ± SD, $P = 0.01$, *t*-test compared to nil), while sham acupuncture did not significantly change conduction latency (0.12 ± 0.51 ms, $P = 0.28$). Based on these results, we further evaluated if either verum acupuncture group individually demonstrated reduced median sensory nerve conduction latency, and found that both local and distal acupuncture reduced latency compared to sham acupuncture ($P = 0.03$ and $P = 0.02$, respectively; single-tailed unpaired *t*-test) and compared to nil (local: −0.16 ± 0.42 ms, $P = 0.048$, single tailed *t*-test; distal: −0.17 ± 0.35 ms, $P = 0.02$, single tailed *t*-test). Reduced median sensory nerve latency following verum acupuncture therapy showed a trending correlation (r = 0.26,

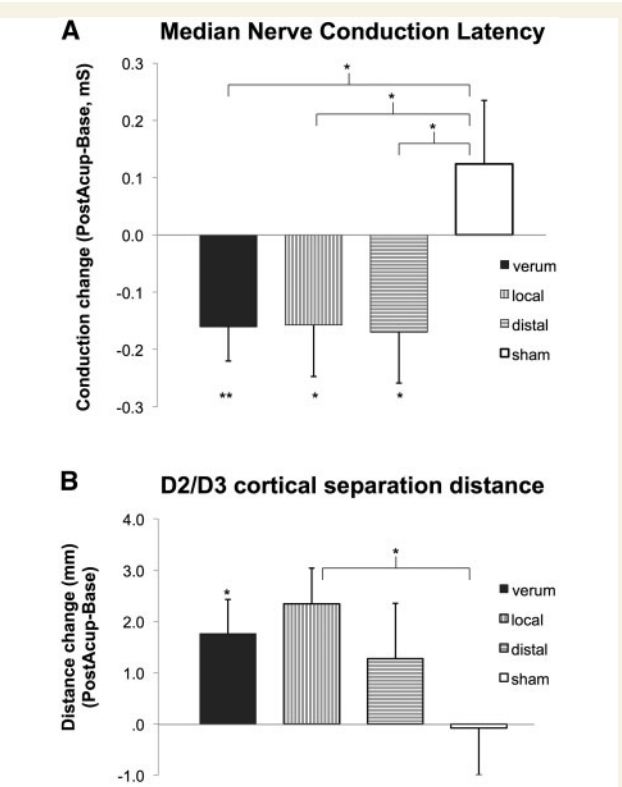

Figure 3 NCS and S1 somatotopy response to therapy. (**A**) Nerve conduction studies of the median sensory nerve demonstrated significant improvement in conduction latency following verum but not sham acupuncture. (**B**) Separation distance of cortical representations in the primary somatosensory cortex for affected digits 2 and 3, as assessed by functional MRI, demonstrated significant increase following verum, but not sham, acupuncture. Note that CTS verum combines results across both CTS-local and CTS-distal study arms. Error bars represent SEM. $^{*}P < 0.05$; $^{**}P < 0.01$.

$P = 0.09$) with % change in BCTQ symptom score. A significant correlation (r = 0.37, $P = 0.03$) between reduced latency following verum acupuncture and BCTQ symptom score at 3-month follow-up was also noted.

Somatosensory cortical mapping with functional MRI

For each subject, the peak vertex for the most significant cluster in S1 was extracted for each digit and cortical separation distance for each digit pair was calculated, with D2/D3 separation serving as primary outcome based on past research (Napadow *et al.*, 2006, 2007*a*; Dhond *et al.*, 2012; Maeda *et al.*, 2014). Due to subject drop-out and technical limitations (e.g. head motion > 3 mm, scanner artefacts, etc.), for either the baseline and/or post-therapy MRI evaluations of the two digits, change in D2/D3 separation distance was calculated for 36 subjects (local: $n = 11$, distal: $n = 13$, sham: $n = 12$). A 2 × 2 repeated measures ANOVA found no significant Group (local, distal acupuncture) × Time (baseline, post-therapy) interaction for verum acupuncture groups [$F(1,22) = 0.64$, $P = 0.43$], and thus local and distal acupuncture groups were combined into a single verum group for subsequent analyses. A repeated measures ANOVA demonstrated a significant Group (verum, sham acupuncture) main effect [$F(1,34) = 7.30$, $P = 0.01$], but no Time (baseline, post-therapy) main effect [$F(1,34) = 2.19$, $P = 0.15$], nor Group × Time interaction [$F(1,34) = 2.64$, $P = 0.11$]. *Post hoc* analysis found trending significance for greater increase in D2/D3 separation distance for verum (post-acupuncture baseline = 1.8 ± 3.2 mm, mean ± SD), compared to sham (−0.1 ± 3.2 mm) acupuncture (unpaired *t*-test, $P = 0.10$), and a significant group difference using % change scores (Mann-Whitney U-test, $P = 0.04$), which were non-normally distributed (Shapiro-Wilk test). Furthermore, D2/D3 separation distance ($P = 0.014$, one-sample *t*-test) and % change ($P = 0.004$, Wilcoxon Signed Rank test) were significantly increased for verum, but not sham ($P = 0.93$; % change: $P = 0.94$) acupuncture. Based on these results, we also evaluated if either verum acupuncture group individually demonstrated increased D2/D3 separation distance compared to sham acupuncture, and found that local (2.3 ± 2.3 mm, $P = 0.02$, one-sample *t*-test; % change: $P = 0.02$, Wilcoxon), but not distal (1.3 ± 3.9 mm, $P = 0.18$; % change: $P = 0.21$) acupuncture, increased D2/D3 separation (Fig. 3 and Table 1).

Exploratory analyses also evaluated D2/D5 ($n = 39$, local: $n = 12$, distal: $n = 14$, sham: $n = 13$) and D3/D5 ($n = 40$, local: $n = 14$, distal: $n = 13$, sham: $n = 13$) S1 separation distance, and found that verum acupuncture also increased D2/D5 distance (1.8 ± 4.5 mm, mean ± SD, $P = 0.047$, one-sample *t*-test; % change: $P = 0.02$) but not D3/D5 distance (0.4 ± 4.4, $P = 0.68$; % change: $P = 0.29$), while sham did not change either metric (D2/D5: −0.1 ± 3.0, $P = 0.88$, % change: $P = 0.92$; D3/D5: −0.6 ± 2.6, $P = 0.42$, % change: $P = 0.35$).

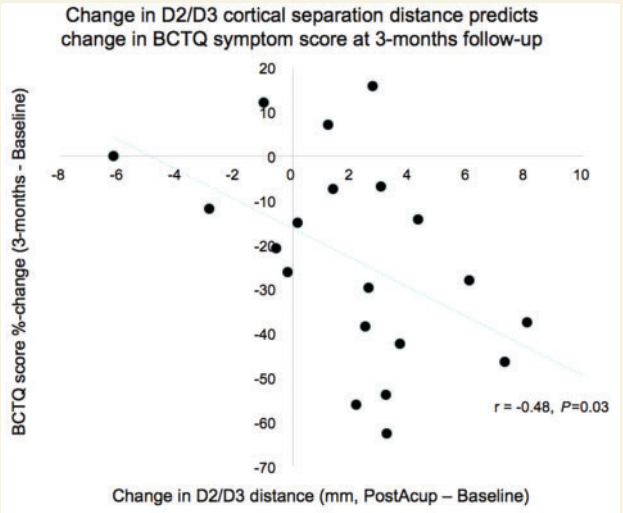

Figure 4 S1 somatotopy response predicts clinical response. Change in S1 cortical separation distance for affected digits 2 and 3 immediately following verum acupuncture was negatively correlated with change in symptom severity assessed by BCTQ at 3-month follow-up, demonstrating capacity of S1 neuroplasticity metrics to predict long-term clinical outcomes following acupuncture therapy for CTS.

We then investigated whether changes in D2/D3 separation distance following verum acupuncture were associated with post-therapy or 3-month follow-up CTS clinical outcomes. We found that change in D2/D3 separation distance was negatively correlated with % change in BCTQ symptom score at 3-month follow-up (r = −0.48, $P = 0.03$, Fig. 4). This association also existed for % change in D2/D3 separation (Spearman rho = −0.51, $P = 0.02$). Change in D2/D3 separation (r = 0.10, $P = 0.65$; or % change, rho = 0.13, $P = 0.58$) was not associated with % change in BCTQ symptom score immediately after therapy.

Assessment of S1-adjacent white matter microstructure with diffusion tensor imaging

To better understand the mechanisms by which different forms of acupuncture improve CTS clinical outcomes, we also evaluated white matter microstructure adjacent to S1 using a masked-skeleton analysis. First, we found that compared to healthy adults, CTS patients demonstrate increased fractional anisotropy within four distinct clusters along the white matter skeleton adjacent to: (i) S1-hand area contralesional to the more affected CTS hand [$x = -34.2$, $y = -27.8$, $z = 44.5$; FWE corrected $P < 0.05$, threshold-free cluster enhancement (TFCE)]; (ii) S1-hand area ipsilesional to the more affected hand ($x = 40.0$,

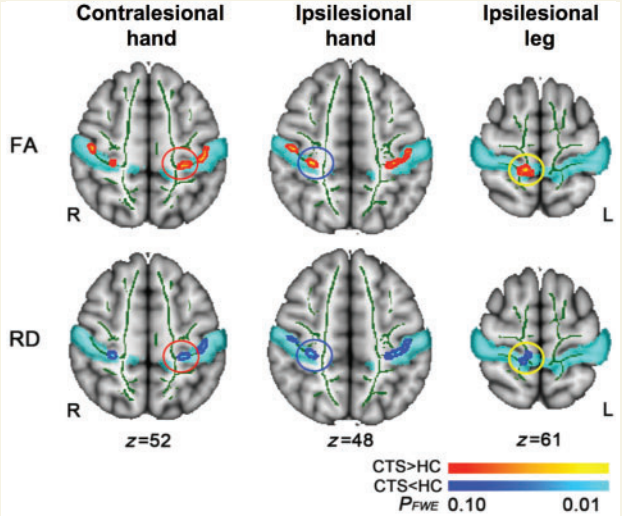

Figure 5 S1-adjacent white matter microstructure differs between CTS and healthy control subjects. DTI analyses of white matter adjacent to S1 showed increased fractional anisotropy (FA) and correspondingly reduced radial diffusivity (RD) in both contralesional and ipsilesional hand areas, and ipsilesional leg area, for CTS compared to healthy controls (HC).

$y = -22.0$, $z = 45.7$); (iii) S1-leg area ipsilesional to the more affected hand ($x = 11.8$, $y = -38.2$, $z = 60.9$); and (iv) S1-face area contralesional to the more affected hand ($x = -49.5$, $y = -16.7$, $z = 35.7$) (Fig. 5). The S1 masked skeleton analysis also found that compared to healthy adults, CTS patients demonstrated reduced radial diffusivity in a similar S1 ipsilesional hand and leg area (FWE corrected $P < 0.05$, TFCE). There was also a trend (FWE corrected $P < 0.08$, TFCE) for reduced radial diffusivity in an S1-hand area contralesional to the more affected CTS hand (similar in location to the region with increased fractional anisotropy, above). No significant group differences for mean or axial diffusivity were noted.

We thereafter assessed fractional anisotropy and radial diffusivity changes following therapy. As age significantly correlated with mean fractional anisotropy and radial diffusivity in the skeleton at baseline ($r = -0.39$; $P = 0.002$; $r = 0.44$, $P < 0.001$, respectively) but sex did not ($P = 0.33$, $P = 0.68$, respectively), subsequent analyses used a repeated measures ANCOVA (factors Cluster, Time and Group), controlling for age. For fractional anisotropy, there was no significant Cluster (four S1 areas) × Group (verum, sham acupuncture) × Time (baseline, post-therapy) interaction [$F(2.6,142.9) = 1.17$; $P = 0.32$] nor Group × Time interaction [$F(1,55) = 1.67$; $P = 0.20$]. For radial diffusivity there was also no significant Cluster × Group × Time interaction [$F(2.7,148.1) = 1.73$; $P = 0.17$] nor Group × Time interaction [$F(1,55) = 0.11$; $P = 0.74$]. We then investigated if interindividual differences in fractional anisotropy changes following therapy were associated with improvements in median sensory nerve conduction latency (Fig. 6). For the contralesional S1-hand area cluster, we found a significant correlation between fractional anisotropy and median sensory nerve latency changes ($r = 0.37$, $P = 0.03$) after verum acupuncture. Fractional anisotropy change after sham acupuncture showed no correlation with latency change ($r = 0.26$, $P = 0.28$). Interestingly, for the ipsilesional hand area cluster, we found a significant correlation between changes in fractional anisotropy and median sensory nerve latency changes ($r = 0.46$, $P = 0.04$) after local, but not after distal ($r = 0.05$, $P = 0.87$) or sham ($r = -0.01$, $P = 0.96$) acupuncture. In contrast, for the ipsilesional leg area cluster, we found a significant correlation between changes in fractional anisotropy and median sensory nerve latency changes ($r = 0.56$, $P = 0.03$) only after distal, and not local ($r = 0.09$, $P = 0.72$) or sham ($r = 0.33$, $P = 0.16$) acupuncture. For the S1-face area cluster, there were no significant correlations for any therapy group. Additionally, no significant correlations for changes in radial diffusivity were noted.

Discussion

Our randomized controlled neuroimaging trial evaluated S1 neuroplasticity supporting acupuncture mechanisms for CTS. We found that while both verum and sham acupuncture reduced CTS symptoms, verum was superior to sham in producing improvements in neurophysiological outcomes, both local to the wrist (i.e. median sensory nerve conduction latency) and central (i.e. D2/D3 S1 cortical separation distance in the brain). In fact, while both D2/D3 and D2/D5 were increased by verum acupuncture, D3/D5 was not, suggesting that D2 shifted ventrally along S1, away from both D3 and D5. Furthermore, greater improvement in D2/D3 separation following verum acupuncture predicted sustained improvement in symptom severity at 3-month follow-up, thus linking improvements in S1 somatotopy with long-term clinical outcomes. Interestingly, verum acupuncture at distal sites on the lower leg contralesional to the more affected hand also reduced symptoms and was superior to sham acupuncture in improving median nerve conduction latency. DTI of S1-adjacent white matter found increased fractional anisotropy and reduced radial diffusivity in CTS near bilateral hand areas and ipsilesional leg area compared to healthy control subjects. Longitudinal results demonstrated that improvement in median nerve latency was associated with reduced fractional anisotropy near (i) contralesional S1-hand area following verum, but not sham, acupuncture; (ii) ipsilesional S1-hand area following local, but not distal or sham, acupuncture; and (iii) ipsilesional S1-leg area following distal, but not local or sham, acupuncture. As these S1 subregions are distinctly targeted by local versus distal acupuncture electrostimulation, acupuncture at local versus distal sites may improve median nerve function at the wrist by somatotopically distinct S1-mediated neuroplasticity following therapy.

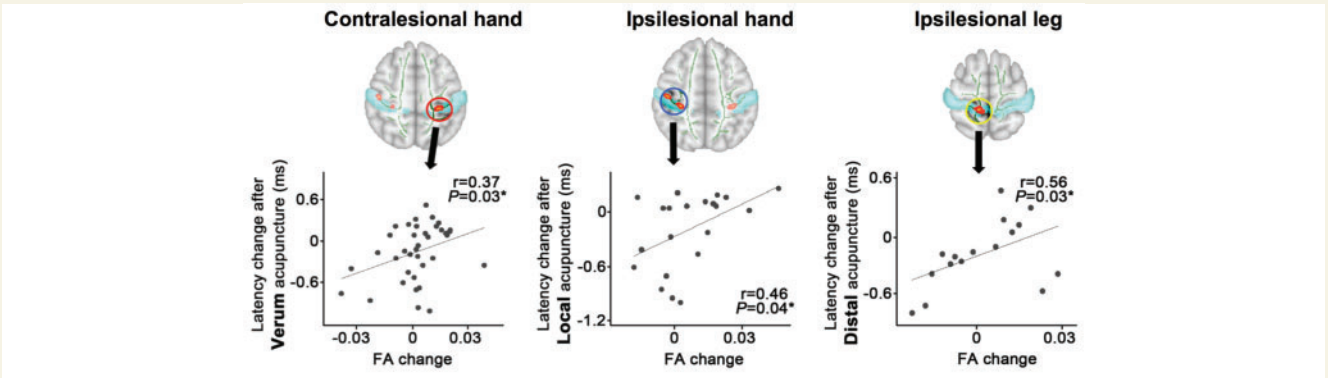

Figure 6 Post-therapy improvement in nerve conduction studies is associated with somatotopically-specific post-therapy improvements in white matter microstructure. Longitudinal DTI analyses demonstrated somatotopic specificity for improvements following acupuncture therapy at distinct body sites (i.e. local versus distal acupuncture therapy arms). Specifically, reduction in median nerve latency was associated with decreased fractional anisotropy (FA) near (i) contralesional hand area following verum, but not sham, acupuncture; (ii) ipsilesional hand area following local, but not distal or sham, acupuncture; and (iii) ipsilesional leg area following distal, but not local or sham, acupuncture.

Following up on our pilot acupuncture neuroimaging study for CTS (Napadow *et al.*, 2007*b*), this study is the first sham controlled neuroimaging acupuncture study for CTS. Other acupuncture clinical trials for CTS (Yao *et al.*, 2012), similar to our study, found no difference between verum and sham acupuncture for symptom reduction—a subjective/psychological outcome. However, our results demonstrate that objective/physiological outcomes (both at the wrist and in the brain) do show specific improvement for verum acupuncture. Controversy persists as to whether or not acupuncture differs from placebo. Sham acupuncture, which certainly imparts afference via cutaneous receptors and subsequent brain response (Huang *et al.*, 2012) may, as a sham device coupled with specific ritual, produce a stronger placebo effect than a placebo-drug pill, for instance (Linde *et al.*, 2010). In fact, our results may be analogous to a sham-controlled study of albuterol inhaler for asthma, which demonstrated that while sham acupuncture and placebo inhaler was as effective as an albuterol inhaler in terms of symptom reduction, objective physiological outcomes (i.e. spirometry to assess forced expiratory volume) did demonstrate significant improvement for albuterol (Wechsler *et al.*, 2011); the authors suggested that patient self-report of symptom severity may be less reliable from a clinical management standpoint compared to objective physiological outcomes. Chronic pain disorders similarly lack established biomarkers or objective outcomes (Tracey, 2011). However, for CTS, a neuropathic pain disorder, local peripheral nerve outcomes are well established and candidate S1-based outcomes have also been described. Our results suggest that such outcomes may be less susceptible to sham acupuncture, which may instead modulate known placebo circuitry (e.g. prefrontal cortex, ventral striatum etc.) (Wager *et al.*, 2015). In turn, median nerve conduction and S1 neuroplasticity may be more sensitive to electro-acupuncture interventions that do provide more prolonged (compared to sham acupuncture) and regulated afference to the brain.

Interestingly, while local and distal acupuncture therapy did not differ in post-treatment change in median nerve conduction latency (and both showed improvements relative to sham acupuncture), the mechanisms supporting these improvements may be associated with distinct, somatotopically-mediated plasticity in S1-adjacent white matter (Fig. 7). Specifically, for CTS patients treated with local acupuncture, improvements in median nerve latency were associated with reduction of fractional anisotropy, a DTI measure of white matter integrity, near ipsilesional S1-hand area. In contrast, for CTS patients treated with distal acupuncture, improvements in median nerve latency were instead associated with reduction of fractional anisotropy near ipsilesional S1-leg area. A baseline comparison found that CTS patients showed increased fractional anisotropy in these S1-adjacent areas compared to healthy control subjects, with concomitantly decreased radial diffusivity in the same areas, suggesting that increased diffusion anisotropy was due to reduced diffusion perpendicular to principle white matter fibre direction. While the interpretation of such changes is not well understood, it may be compensatory, e.g. increased myelination (Beaulieu, 2002) as a form of maladaptive neuroplastic response to CTS-associated afference. Neuronal activity can regulate myelination in the brain (Baraban *et al.*, 2016), and reduced radial diffusivity and increased fractional anisotropy is consistent with increased myelination, with the latter noted in human and animal models of learning (Blumenfeld-Katzir *et al.*, 2011; Zatorre *et al.*, 2012). Thus, fractional anisotropy reductions (e.g. in S1-adjacent white matter for CTS) may be beneficial, and have been noted following sensorimotor training in musicians, ballet dancers, and car racing

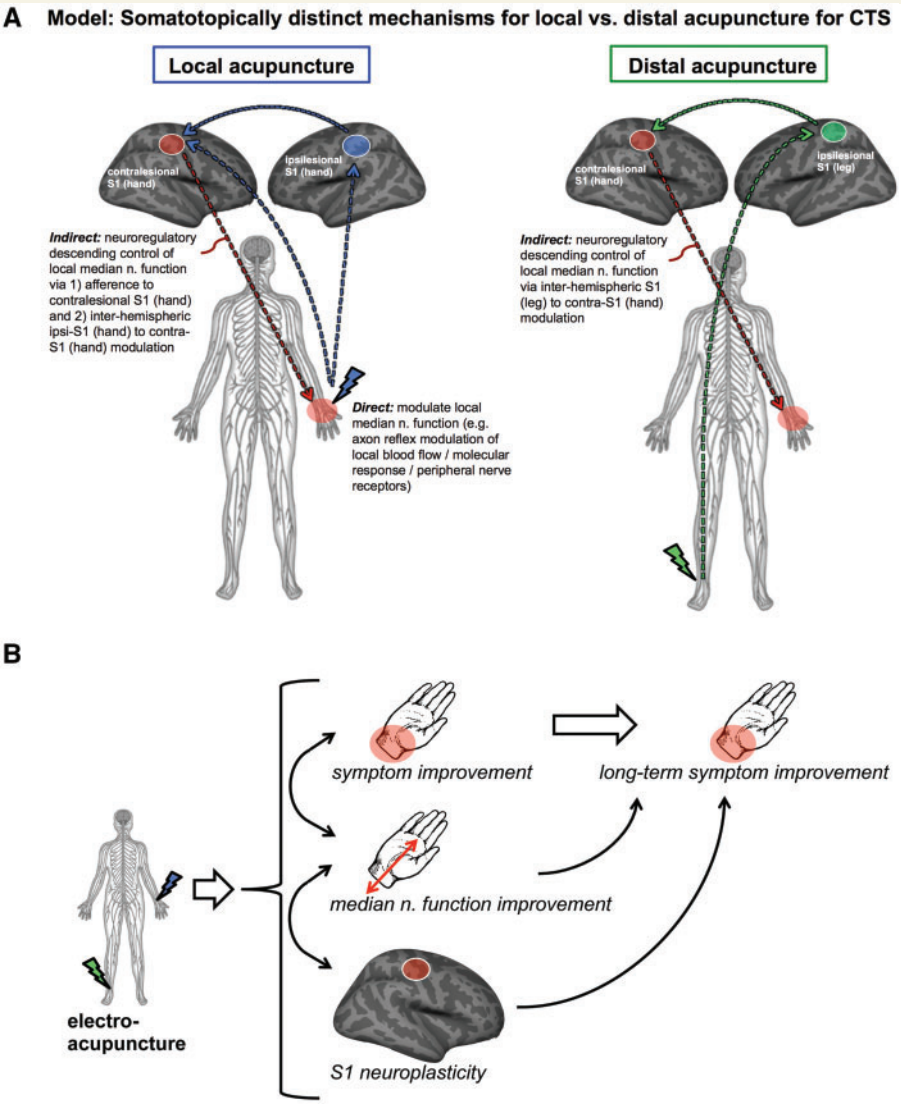

Figure 7 Schematic summarizing CTS response to acupuncture therapy. (**A**) While distal acupuncture at the leg can modulate median nerve function via indirect S1 interhemispheric neuroregulatory pathways, local acupuncture can modulate median nerve function at the wrist via both indirect (e.g. S1 influences on the central autonomic control of local vasa nervorum) and direct pathways (e.g. direct axon reflex mediated control of local vasa nervorum). (**B**) Our results demonstrate that electro-acupuncture can produce improvement in symptoms, median nerve function, and S1 neuroplasticity, with objective changes following therapy (median nerve function, functional S1 neuroplasticity) directly predicting long-term symptom improvement.

gamers (Imfeld *et al.*, 2009; Hanggi *et al.*, 2010; Hofstetter *et al.*, 2013). In our study, improvements in median nerve latency following acupuncture were indeed associated with reduced fractional anisotropy in S1-adjacent white matter. While speculative, repetitive electrical stimulation in verum acupuncture may reduce white matter myelination, though other mechanisms may also play a role (e.g. axonal membrane, glial morphometry changes) to reduce fractional anisotropy and increase radial diffusivity in conjunction with beneficial changes in peripheral median nerve function (Beaulieu, 2002).

Our previous functional MRI results showed that while ipsilesional S1-hand area is deactivated by local acupuncture, ipsilesional S1-leg area is activated by distal acupuncture (Maeda *et al.*, 2013*b*). Thus, clinically-relevant fractional anisotropy changes for both local and distal acupuncture were not diffusely distributed throughout S1-adjacent white matter, but were instead localized to areas adjacent to S1 subregions specifically targeted by wrist versus leg acupuncture. Notably, a combined sample of local and distal acupuncture treated CTS patients showed that improvement in median nerve latency was associated with reduction of fractional anisotropy near contralesional S1-hand area following therapy. Hence, fractional anisotropy reduction in this contralesional region likely plays a role in the common pathway for both groups in

neuroregulatory control of peripheral nerve function in CTS (Fig. 7). Notably, while the associations between fractional anisotropy change and changes in median nerve latency were provocative, we did not find group-level improvements (i.e. reduction) in fractional anisotropy following acupuncture for any group. The lack of fractional anisotropy reduction on a group level may have been due to a longer duration of time required for structural, in this case white matter, plasticity. Hence, correlations between median nerve latency improvements and fractional anisotropy reduction may have been driven by a subset of highly responsive patients with faster changes in white matter microstructure. Furthermore, while local acupuncture increased cortical representation D2/D3 separation distance in contralesional S1-hand area, distal acupuncture did not, suggesting that functional cortical re-mapping is downstream of peripheral nerve changes, as both local and distal acupuncture improved nerve conduction study outcomes, and that, similar to above, a longer duration of time is also required for functional plasticity following peripheral nerve improvements. Future longitudinal studies should sample imaging outcomes at a greater number of time points and determine the temporal order of peripheral versus central changes following acupuncture therapy.

While the mechanism by which brain-based plasticity might influence median nerve function in CTS is unknown, possibilities include central autonomic control of the vascular tone for arterioles feeding the vasa nervorum of the median nerve, as intraneural blood flow is known to be controlled by sympathetic innervation (Lundborg, 1988). In fact, a recent neuroimaging meta-analysis noted S1 as part of a network of brain regions regulating autonomic, particularly sympathetic, outflow (Beissner *et al.*, 2013). In addition, our recent study in patients with chronic pain found that pain-evoked increase in S1 connectivity to the anterior/middle insula cortex was associated with reduced cardiovagal modulation (Kim *et al.*, 2015). These studies link S1 with central control of autonomic tone and future studies should explore if, for example, S1-insula connectivity is also associated with both autonomic (e.g. sympathetic) and median nerve conduction response to acupuncture in CTS patients. Another mechanism by which acupuncture, particularly local acupuncture, modulates median nerve vasa nervorum blood flow may be via antidromic vasodilation following stimulation of spinal dorsal roots–an effect mediated by calcitonin gene-related peptide (Sato *et al.*, 1994, 2000). Ultrasound studies have explored median nerve hypervascularity (Ghasemi-Esfe *et al.*, 2011; Ooi *et al.*, 2014), a compensatory response to ischaemia within the tunnel, and future studies should link median nerve vascularity with neuroplasticity response to acupuncture therapy.

We also found that CTS symptom reduction persists 3 months after cessation of verum acupuncture therapy. These improvements are in-line with previous clinical trials of acupuncture for CTS (Yang *et al.*, 2011), which reported lasting improvements for both symptoms and nerve conduction latencies, and suggests that brain neuroplasticity following therapy can also be sustained. Interestingly, we found that cortical D2/D3 separation increase following verum acupuncture predicted sustained reduction in symptom severity at 3-month follow-up, thus linking improvements in S1 somatotopy with prediction of long-term clinical outcomes. The fact that symptom severity reduction immediately after verum acupuncture did not correlate with D2/D3 separation improvements suggests a more gradual mechanism by which S1 cortical plasticity steadily affects plasticity in other brain regions that play an important role in determining symptom severity ratings, such as prefrontal cognitive and limbic affective brain regions. Alternatively, S1 plasticity may require time to affect median nerve function, potentially by the central autonomic control pathways noted above, and future studies should also assess long-term changes in median nerve conduction latencies to better understand the interrelatedness of plasticity in the central and peripheral nervous system with patient reported symptom outcomes.

Limitations to our study should be noted. Due to the duration of therapy and human subjects research ethics board stipulations, subjects were un-blinded as to treatment group following post-therapy MRI scan session, potentially confounding our finding of worsening symptom severity for sham acupuncture at 3-month follow-up. Therefore, links to long-term clinical outcomes were restricted to the verum group only. Reduced symptom severity following verum acupuncture was found to be maintained 3-months following therapy, consistent with prior clinical trials (Yang *et al.*, 2011), and our data demonstrated that such long-term relief may depend on successful reversal of maladaptive plasticity in S1, i.e. D2/D3 separation distance (an objective measure). Thus, un-blinding post-therapy may not have confounded the verum as much as sham acupuncture arm. In addition, we did not correct for multiple regions of interest in our analyses linking nerve conduction study changes with longitudinal changes in DTI metrics. However, these regions of interest were localized in white matter adjacent to distinct somatotopically-defined subregions of S1. Thus, we made regionally-bounded hypotheses for these comparisons as regions of interest were differentially targeted by different acupuncture intervention groups, allowing for a region of interest-specific hypothesis for each group.

In conclusion, while both verum and sham acupuncture reduced CTS symptoms, verum acupuncture was superior to sham in producing improvements in both peripheral and brain neurophysiological outcomes. Furthermore, improvement in functional S1 plasticity immediately following acupuncture predicted long-term symptom relief. Interestingly, DTI analysis of white matter microstructure found that acupuncture at local versus distal acupuncture sites may improve median nerve function at the wrist by somatotopically distinct S1-mediated neuroplasticity following therapy. Our study suggests that acupuncture may improve

CTS pathophysiology by both local and brain-based mechanisms involving S1 neuroplasticity.

Funding

This research was supported by the National Center for Complementary and Integrative Health (NCCIH), U.S. National Institutes of Health (NIH) (R01-AT004714, R01-AT004714-02S1, P01-AT006663, K24-AT004095), Korean Institute of Oriental Medicine (KIOM) (C16210), as well as the National Center for Research Resources (NCRR) NIH (P41-RR14075, S10-RR021110, S10-RR023043)

Supplementary material

Supplementary material is available at *Brain* online.

References

Atroshi I, Gummesson C, Johnsson R, Ornstein E, Ranstam J, Rosen I. Prevalence of carpal tunnel syndrome in a general population. JAMA 1999; 282: 153–8.

Baraban M, Mensch S, Lyons DA. Adaptive myelination from fish to man. Brain Res 2016; 1641(Pt A): 149–61.

Beaulieu C. The basis of anisotropic water diffusion in the nervous system - a technical review. NMR Biomed 2002; 15: 435–55.

Beissner F, Meissner K, Bar KJ, Napadow V. The autonomic brain: an activation likelihood estimation meta-analysis for central processing of autonomic function. J Neurosci 2013; 33: 10503–11.

Blumenfeld-Katzir T, Pasternak O, Dagan M, Assaf Y. Diffusion MRI of structural brain plasticity induced by a learning and memory task. PLoS One 2011; 6: e20678.

Dhond R, Ruzich E, Witzel T, Maeda Y, Malatesta C, Morse L, et al. Spatiotemporal mapping cortical neuroplasticity in carpal tunnel syndrome. Brain 2012; 135(Pt 10): 3062–73.

Douaud G, Jbabdi S, Behrens TE, Menke RA, Gass A, Monsch AU, et al. DTI measures in crossing-fibre areas: increased diffusion anisotropy reveals early white matter alteration in MCI and mild Alzheimers disease. Neuroimage 2011; 55: 880–90.

Douaud G, Mackay C, Andersson J, James S, Quested D, Ray MK, et al. Schizophrenia delays and alters maturation of the brain in adolescence. Brain 2009; 132(Pt 9): 2437–48.

Druschky K, Kaltenhauser M, Hummel C, Druschky A, Huk WJ, Stefan H, et al. Alteration of the somatosensory cortical map in peripheral mononeuropathy due to carpal tunnel syndrome. Neuroreport 2000; 11: 3925–30.

Durkan JA. A new diagnostic test for carpal tunnel syndrome. J Bone Joint Surg Am 1991; 73: 535–8.

Engvig A, Fjell AM, Westlye LT, Moberget T, Sundseth O, Larsen VA, Walhovd KB. Memory training impacts short-term changes in aging white matter: a longitudinal diffusion tensor imaging study. Hum Brain Mapp 2012; 33: 2390–406.

Famm K, Litt B, Tracey KJ, Boyden ES, Slaoui M. Drug discovery: a jump-start for electroceuticals. Nature 2013; 496: 159–61.

Farrar JT, Young JP, LaMoreaux L, Jr.Werth JL, Poole RM. Clinical importance of changes in chronic pain intensity measured on an 11-point numerical pain rating scale. Pain 2001; 94: 149–58.

Ghasemi-Esfe AR, Khalilzadeh O, Mazloumi M, Vaziri-Bozorg SM, Niri SG, Kahnouji H, Rahmani M. Combination of high-resolution and color Doppler ultrasound in diagnosis of carpal tunnel syndrome. Acta Radiol 2011; 52: 191–7.

Greve DN, Fischl B. Accurate and robust brain image alignment using boundary-based registration. Neuroimage 2009; 48: 63–72.

Hanggi J, Koeneke S, Bezzola L, Jancke L. Structural neuroplasticity in the sensorimotor network of professional female ballet dancers. Hum Brain Mapp 2010; 31: 1196–206.

Hanley MA, Jensen MP, Ehde DM, Robinson LR, Cardenas DD, Turner JA Smith DG. Clinically significant change in pain intensity ratings in persons with spinal cord injury or amputation. Clin J Pain 2006; 22: 25–31.

Hofstetter S, Tavor I, Tzur Moryosef S, Assaf Y. Short-term learning induces white matter plasticity in the fornix. J Neurosci 2013; 33: 12844–50.

Huang W, Pach D, Napadow V, Park K, Long X, Neumann J, Maeda Y, Nierhaus T, Liang F, Witt CM. Characterizing acupuncture stimuli using brain imaging with FMRI–a systematic review and meta-analysis of the literature. PLoS One 2012; 7: e32960.

Imfeld A, Oechslin MS, Meyer M, Loenneker T Jancke L. White matter plasticity in the corticospinal tract of musicians: a diffusion tensor imaging study. Neuroimage 2009; 46: 600–7.

Jenkinson M, Bannister P, Brady M Smith S. Improved optimization for the robust and accurate linear registration and motion correction of brain images. Neuroimage 2002; 17: 825–41.

Jenkinson M, Beckmann CF, Behrens TE, Woolrich MW Smith SM. Fsl. Neuroimage 2012; 62: 782–90.

Jensen MP, Chen C, Brugger AM. Interpretation of visual analog scale ratings and change scores: a reanalysis of two clinical trials of postoperative pain. J Pain 2003; 4: 407–14.

Kaptchuk TJ. Acupuncture: theory, efficacy, and practice. Ann Intern Med 2002; 136: 374–383.

Khosrawi S, Moghtaderi A, Haghighat S. Acupuncture in treatment of carpal tunnel syndrome: a randomized controlled trial study. J Res Med Sci 2012; 17: 1–7.

Kim J, Loggia ML, Cahalan CM, Harris RE, Beissner F, Garcia RG, et al. The somatosensory link in fibromyalgia: functional connectivity of the primary somatosensory cortex is altered by sustained pain and is associated with clinical/autonomic dysfunction. Arthritis Rheumatol 2015; 67: 1395–405.

Kleopa KA. In the Clinic. Carpal Tunnel Syndrome. Ann Intern Med 2015; 163: ITC1.

Kong J, Gollub R, Huang T, Polich G, Napadow V, Hui K, Vangel M, Rosen B, Kaptchuk TJ. Acupuncture de qi, from qualitative history to quantitative measurement. J Altern Complement Med 2007; 13: 1059–70.

Langevin HM, Schnyer R, MacPherson H, Davis R, Harris RE, Napadow V, et al. Manual and electrical needle stimulation in acupuncture research: pitfalls and challenges of heterogeneity. J Altern Complement Med 2015; 21: 113–28.

Levine DW, Simmons BP, Koris MJ, Daltroy LH, Hohl GG, Fossel AH, Katz JN. A self-administered questionnaire for the assessment of severity of symptoms and functional status in carpal tunnel syndrome. J Bone Joint Surg Am 1993; 75: 1585–92.

Linde K, Niemann K Meissner K. Are sham acupuncture interventions more effective than (other) placebos? A re-analysis of data from the Cochrane review on placebo effects. Forsch Komplementmed 2010; 17: 259–64.

Lundborg G. Intraneural microcirculation. Orthop Clin North Am 1988; 19: 1–12.

Ma D, Liveson J. Nerve Conduction Handbook. Philadelphia, FA Davis Co, 1983.

Maeda Y, Kettner N, Holden J, Lee J, Kim J, Cina S, et al. Functional deficits in carpal tunnel syndrome reflect reorganization of primary somatosensory cortex. Brain 2014; 137(Pt 6): 1741–52.

Maeda Y, Kettner N, Kim J, Kim H, Cina S, Malatesta C, et al. Primary somatosensory/motor cortical thickness distinguishes paresthesia-dominant from pain-dominant carpal tunnel syndrome. Pain 2016; 157: 1085–93.

Maeda Y, Kettner N, Lee J, Kim J, Cina S, Malatesta C, et al. Acupuncture evoked response in contralateral somatosensory cortex reflects peripheral nerve pathology of carpal tunnel syndrome. Med Acupunct 2013a; 25: 275–84.

Maeda Y, Kettner N, Sheehan J, Kim J, Cina S, Malatesta C, et al. Altered brain morphometry in carpal tunnel syndrome is associated with median nerve pathology. Neuroimage (Amst) 2013b; 2: 313–9.

Napadow V, Kettner N, Liu J, Li M, Kwong KK, Vangel M, et al. Hypothalamus and amygdala response to acupuncture stimuli in Carpal Tunnel Syndrome. Pain 2007a; 130: 254–66.

Napadow V, Kettner N, Ryan A, Kwong KK, Audette J, Hui KK. Somatosensory cortical plasticity in carpal tunnel syndrome–a cross-sectional fMRI evaluation. Neuroimage 2006; 31: 520–30.

Napadow V, Liu J, Li M, Kettner N, Ryan A, Kwong KK, et al. Somatosensory cortical plasticity in carpal tunnel syndrome treated by acupuncture. Hum Brain Mapp 2007b; 28: 159–71.

Neal S, Fields KB. Peripheral nerve entrapment and injury in the upper extremity. Am Fam Physician 2010; 81: 147–55.

NIH. NIH Consensus Conference. Acupuncture. Jama 1998; 280: 1518–24.

Ooi CC, Wong SK, Tan AB, Chin AY, Abu Bakar R, Goh SY, et al. Diagnostic criteria of carpal tunnel syndrome using high-resolution ultrasonography: correlation with nerve conduction studies. Skeletal Radiol 2014; 43: 1387–94.

Papanicolaou GD, McCabe SJ Firrell J. The prevalence and characteristics of nerve compression symptoms in the general population. J Hand Surg [Am] 2001; 26: 460–6.

Phalen GS. The carpal-tunnel syndrome. Seventeen years experience in diagnosis and treatment of six hundred fifty-four hands. J Bone Joint Surg Am 1966; 48: 211–28.

Sato A, Sato Y, Shimura M Uchida S. Calcitonin gene-related peptide produces skeletal muscle vasodilation following antidromic stimulation of unmyelinated afferents in the dorsal root in rats. Neurosci Lett 2000; 283: 137–40.

Sato A, Sato Y, Uchida S. Blood flow in the sciatic nerve is regulated by vasoconstrictive and vasodilative nerve fibers originating from the ventral and dorsal roots of the spinal nerves. Neurosci Res 1994; 21: 125–33.

Sim H, Shin BC, Lee MS, Jung A, Lee H, Ernst E. Acupuncture for carpal tunnel syndrome: a systematic review of randomized controlled trials. J Pain 2011; 12: 307–14.

Smith SM, Jenkinson M, Johansen-Berg H, Rueckert D, Nichols TE, Mackay CE, et al. Tract-based spatial statistics: voxelwise analysis of multi-subject diffusion data. Neuroimage 2006; 31: 1487–505.

Tecchio F, Padua L, Aprile I Rossini PM. Carpal tunnel syndrome modifies sensory hand cortical somatotopy: a MEG study. Hum Brain Mapp 2002; 17: 28–36.

Tracey I. Can neuroimaging studies identify pain endophenotypes in humans? Nat Rev Neurol 2011; 7: 173–81.

Wager TD, Atlas LY. The neuroscience of placebo effects: connecting context, learning and health. Nat Rev Neurosci 2015; 16: 403–418.

Waltz E. A spark at the periphery. Nat Biotechnol 2016; 34: 904–8.

Wechsler ME, Kelley JM, Boyd IO, Dutile S, Marigowda G, Kirsch I, et al. Active albuterol or placebo, sham acupuncture, or no intervention in asthma. N Engl J Med 2011; 365: 119–26.

Winkler AM, Ridgway GR, Webster MA, Smith SM, Nichols TE. Permutation inference for the general linear model. Neuroimage 2014; 92: 381–97.

Yang CP, Hsieh CL, Wang NH, Li TC, Hwang KL, Yu SC, et al. Acupuncture in patients with carpal tunnel syndrome: a randomized controlled trial. Clin J Pain 2009; 25: 327–33.

Yang CP, Wang NH, Li TC, Hsieh CL, Chang HH, Hwang KL, et al. A randomized clinical trial of acupuncture versus oral steroids for carpal tunnel syndrome: a long-term follow-up. J Pain 2011; 12: 272–9.

Yao E, Gerritz PK, Henricson E, Abresch T, Kim J, Han J, et al. Randomized controlled trial comparing acupuncture with placebo acupuncture for the treatment of carpal tunnel syndrome. PM R 2012; 4: 367–73.

Zatorre RJ, Fields RD, Johansen-Berg H. Plasticity in gray and white: neuroimaging changes in brain structure during learning. Nat Neurosci 2012; 15: 528–36.